 doi:10.20944/preprints202102.0363.v2

Article

Design floods considering the epistemic uncertainty

Radu Drobot [1,*], Aurelian Florentin Draghia [2], Daniel Ciuiu [3,4] and Romică Trandafir [3]

[1] Technical University of Civil Engineering, Bucharest, Department of Hydrotechnical Engineering; radu.drobot@utcb.ro
[2] Roua Soft SRL; draghia_aurelian@yahoo.com
[3] Technical University of Civil Engineering, Bucharest, Department of Mathematics; daniel.ciuiu@utcb.ro, romica.trandafir@gmail.com
[4] Centre of Macroeconomic Modelling, National Institute of Economic Research "Costin C. Kiritescu", Romanian Academy; daniel.ciuiu@utcb.ro
* Correspondence: radu.drobot@utcb.ro

Abstract: The design flood concept (DF) provides for an essential tool in designing the hydraulic works, in defining the reservoir operation programs and for a reliable flood hazard identification. Under a simplified approach, the maximum discharge and the floods volume are statistically processed to reasonably define the DF. Yet, the integral hydrograph provides additional key temporal and quantitative details of important significance for flood management and particularly for the reservoirs operation and associated risks of failures. The procedure presented in this paper (as applied on a set of compatibly shaped hydrographs) involves the following key stages: (i) normalize the floods, (ii) define similar flood shape classes and (iii) evaluate the average dimensionless flood (ADF) for each class. The ADFs are finally transformed into a set of (DF)s. Many statistical distributions approximate acceptably the frequent values of the maximum discharges or the flood volumes, yet displaying a significant spread for medium or rare probabilities of exceedance (PE). This scattering, which can be explained by the epistemic uncertainty, defines an area of uncertainty both for measured and extrapolated values. In considering upper and lower values of the uncertainty intervals as limits for maximum discharges and flood volumes, then by combining them compatibly, a set of DFs - as completely defined hydrographs, with different shapes - results for each PE. The herein proposed procedure defines both one peak DF and multi-peaks DF. Subsequently, such DFs do assist water managers in examining and establishing tailored approaches for a variety of input hydrographs. Among the DFs that would correspond to a same PE, the most compact floods arise a special interest, for they are basic in defining the set of safe operation rules for hydraulic structures.

Keywords: Annual Maximum Series; Peak Over Threshold; uncertainty interval; flood parameters; compactness coefficient; flood shape.

1. Introduction

1.1. Parameters of the Design Flood (DF)

The *Design Flood* (also called *Synthetic Flood*) represents the maximum flood that a river/ coastal hydraulic structure can safely pass [1] or can guarantee the safety of involved hydraulic structures [2, 3]. The Directive 2007/60/EC of the European Parliament and of the Council of 23 October 2007 established a general framework for the flood risk management in EU countries [4], which requires the DF use as basic information.

The proper DF evaluation shall reliably support the spatial delineation of the flooded areas and corresponding flood risk management, as well as the proper planning and designing of major hydraulic structures (dams, dikes, diversions) or appurtenant structures associated with the water flow (bridges, culverts, drainage systems, pumping stations).

There are different approaches to obtaining the DF [3, 5-7] such as:

Preprints (www.preprints.org) | NOT PEER-REVIEWED | Posted: 13 May 2021 doi:10.20944/preprints202102.0363.v2

a. Empirical formulae, which derive the peak discharge as a function of catchment size and catchment climatic characteristics;
b. Envelope curves of observed floods;
c. Frequency analyses methods for observed floods. Such an analysis can cover in situ or regional data;
d. Joint (peak-volume) design flood methodology, which evaluates the exceedance probability of the DF volume, given a design peak discharge (as based on a regional approach);
e. Rainfall-based methods: (i) the *design event*–based models consider that the probability of exceedance $P\%$ of the design flood is equal to the probability of exceedance of the input rainfall (assumption valid for small catchments); (ii) in *the joint probability approach,* a deterministic rainfall-runoff model receives probability-distributed inputs to obtain probability-distributed outputs; (iii) *the continuous simulation* uses the recorded or synthetic long-term rainfall, in order to compute the flood hydrographs, which are subsequently subjected to statistical processing.

Depending on the purpose and available data, in the current practice the DF can be defined by: a) maximum discharge, b) set (maximum discharge, flood volume), c) set (maximum discharge, volume, rainfall duration), or d) set (maximum discharge, volume, duration and flood shape). It is certain that the most conclusive results are obtained for a DF, which would represent the entire flood hydrograph.

Usually, the maximum discharge corresponding to different probabilities of exceedance is considered the most important parameter of the Design Flood [5, 8-12]. The maximum discharge is used to establish the dikes height as well as the size of the spillways. However, steady state 2-D hydraulic routing - based on maximum discharges - leads to the simulated largest extension of the flooded areas, for discarding the reductions of the flood volumes and maximum discharges in the downstream reaches, as following the waters captured in the depression areas of the floodplain.

Both above parameters (maximum discharge and flood volume) are being used in establishing the reservoir' reserved volume for flood control and the spillways characteristics. For the case of very large reservoirs (ex.*Three Gorges Dam* [13]), the partial storing of the incoming flood volumes, with corresponding regulating the downstream discharges, is a feasible alternative as well.

The maximum discharge and the flood volume can be processed independently or by considering the bivariate flood frequency analysis [14-23]. At the same time, the copulas (introduced in hydrological research in 2004, by Salvadori & De Michele [24]) overcome the drawbacks of the bivariate distributions [14]. Although key flooding parameters, the set (maximum discharge, flood volume) has proven being inconsistent with the flood risk management through reservoirs. The gradient of the cumulative flood volumes curve is a key element, for it significantly determines the operation of bottom gates and spillways of the dam structure, over the flood duration.

Chuntian et al [25] have introduced – beside the set (peak discharge, flood volume) – the temporal parameter *hydrograph peak time*. Other authors [14, 26-28] have characterized a flood hydrograph by peak, water volume and flood duration, as correlated random variables. Mediero et al. [3] have generated a set of synthetic hydrographs that preserved the statistical characteristics of the observed peaks, volumes and durations, while the hydrograph shape was defined by two variables: the time to peak and the location of the hydrograph centroid.

Brunner et al [17] have characterized the flood events with associated hydrograph parameters: peak discharge, time to peak, duration and flood volume. However, they used only the peak discharge and flood volume for the bivariate return periods, while the flood duration kept as a potential variable. Brunner et al [29] have developed the *Synthetic Design Hydrograph* as based on peak magnitude and flood volume use in frequency analysis and a selected probability density function, in order to model the shape of a normalized recorded hydrograph.

Preprints (www.preprints.org) | NOT PEER-REVIEWED | Posted: 13 May 2021 doi:10.20944/preprints202102.0363.v2

Other authors [30, 31] have included as system variables the following characteristics describing the flow: peak discharge, flood hydrograph shape and event duration, sediment transport rate, volume and concentration and rate of driftwood transport

In Romania the DF (Figure 1) is characterized by 4 main parameters [32, 33]:

a) $Q_{P\%}^{max}$ - maximum discharges corresponding to $P\%$ probability of exceedance

b) T_{peak} - time to peak of the flood hydrograph

c) D - total duration of the flood hydrograph

d) γ - compactness coefficient, which is a parameter that encompasses 3 correlated variables: V, $Q_{P\%}^{max}$ and D.

$$\gamma = \frac{V}{Q_{P\%}^{max} D} \quad (1)$$

where V is the flood volume above the baseflow.

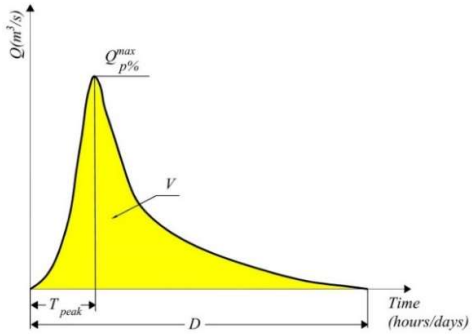

Figure 1. Parameters of the analytic skewed flood hydrograph.

The parameters T_{peak}, D, γ are calculated as the average values of the 4-5 most significant registered floods ranked according to the maximum discharge [32]. A spline function that passes through the points (0, 0), $(T_{peak}, Q_{P\%}^{max})$, $(D, 0)$ and respecting the hydrograph' flood volume shall define the shape of the analytic flood.

1.2. Frequency analysis and statistical tests

Both the discharges and the flood volumes have to be statistically analysed in order to define the DF. The complete data series is rarely used for the statistical processing of the hydrological data. Two methods are employed to select data of interest from the complete series [9, 34-38]:

1. Annual Maximum Series (AMS), the processed data being the annual maximum discharges [5];
2. Partial-duration series or Peak Over Threshold (POT), all events which exceed a predefined value being included in the analysis [5, 39-42].

Prior to any statistical analysis, the hydrological data have to be checked for mutual independence and identical distribution, homogeneity and lack of trend of the sample data. The stationarity of data, although in most of the cases implicitly supposed, is questionable due to land cover and land use changes or of climate change [43, 44]. Statistical tests like Wald-Wolfowitz, Turning point, Mann-Whitney-Wilcoxon and Mann-Kendall are usually used to check if the basic statistical assumptions are fulfilled [10, 45-46].

The empirical distribution of the registered data is fit by different theoretical distributions [5, 35, 47-49]. The most commonly used distributions in hydrology can be divided into four groups [38]: the normal family (normal, log-normal, log-normal type 3), the Generalised Extreme Value (GEV) family (GEV, Gumbel, log-Gumbel, Weibull), the Pearson type 3 (P3) family (Pearson type 3, log-Pearson type 3), and the Generalized Pareto distribution (GP).

Preprints (www.preprints.org) | NOT PEER-REVIEWED | Posted: 13 May 2021 doi:10.20944/preprints202102.0363.v2

According to the selection procedure, the following distributions are preferred [50]:

a) for annual maximum series: GEV, P3, LogPearson3 (LP3), Gamma2, Generalized Gamma, Lognormal distribution (LN) etc.

b) for partial-duration series: Generalized Pareto (GP), Weibull, LP3, Gamma2, Generalized Gamma distribution etc.

The most suitable distribution is selected using goodness-of-fit tests, like Kolmogorov-Smirnov, Anderson-Darling or Chi-Squared tests [46]. While the goodness-of-fit tests respond well for testing the model adequacy when analysing the current floods, they provide an inconsistent adequacy for the hydrograph tail [49]. On the other hand, extreme values are rarely available, while raising uncertainties in the proper evaluation of their empirical PE. Other authors [27, 43] have utilized the root mean square error, Akaike information criterion and Bayesian information criteria, in order to select the most appropriate statistical model.

Following a compatibility comparison of different statistical distributions, one will be selected and considered adequate for a certain aerial region (country). Thus, in the United States, by comparing Lognormal, Gamma, Gumbel, Log-Gumbel, Hazen and Log-Pearson3 the LP3-distribution had been recommended for flood statistical analyses [5]. Australia and Slovenia have opted also for the LP3-distribution; UK prefers GEV and Generalized logistics, while China uses Pearson 3 (P3) distribution [28, 42, 49, 51-52]. P3-distribution was identified as the best distribution for the extrapolation of the regional curves, in the Danube basin [33]. LN and LP3 distributions have been used for the analyses of the Annual Maximum Series for the Danube River [53, 54].

The best distribution to fit the empirical data is rather unknown [6] or could even change in time, as a consequence of aleatory uncertainty, following the time variability and the length of the available maximum discharge series [55-57]. Besides, the recorded data are subject to epistemic uncertainty due to incomplete knowledge of the hydrological system [57-59]. The uncertainty is also present as a result of climate change [60]. It had been noticed that - for the same value of the probability of exceedance $P\%$ - the maximum discharge $Q_{P\%}^{max}$ increases during wet periods, while the same characteristics decrease after a dry period, putting thus into evidence the aleatory uncertainty. The tendency of dry years and wet years to cluster together into longer dry and wet periods is known as the *Hurst phenomenon* [61].

Different probability distributions fit well the empirical values, yet their extrapolation outside the domain of measurements may lead to a large spreading of the estimates (as signalled by many authors [33, 48, 49, 55, 58, 62]). To put into evidence the epistemic uncertainty, Merz and Thieken [55] used 7 distribution functions (GEV, GL - General Logistic, LN3, P3, GUM (Gumbel, GEV type 1), EXP (Exponential) and GP), which all fit well the observed data, while displaying strong differences for data extrapolated values. For the quantification of epistemic uncertainty, Yin et all [52] suggested the use of the confidence intervals of the P3 and GP distributions.

Due to epistemic uncertainty, the statistical estimates belong thus to an uncertainty interval, which will depend on the spreading of the analysed statistical distributions.

Subsequently, instead of using the best distribution function based on additional criteria [55], the uncertainty interval (such as introduced in the present paper) can be capitalized in defining lower and upper reasonable limits of the maximum discharges and flood volumes. Based on these values, a set of flood hydrographs – as corresponding to the same PE - can be obtained. Of them, a special interest is represented by the *compact floods*, which are key elements for flood risk management.

This paper is organized as follows: Section 2 introduces the *Method* used in this study; Section 3 provides *two Case studies*; Section 4 contains *Discussion*, and Section 5 Conclusions.

2. Materials and Methods

The main statistical variables herebelow (maximum discharges and flood volumes) have been processed in order to define the *uncertainty interval*:

Preprints (www.preprints.org) | NOT PEER-REVIEWED | Posted: 13 May 2021 doi:10.20944/preprints202102.0363.v2

- Annual Maximum Series (AMS approach);
- Flood volumes, with selecting those floods whose discharges exceed a specified threshold value (POT approach).

Further, the floods identified above the threshold were used for obtaining the compactness coefficient, the duration and the shape of the DF.

2.1. Maximum annual discharges

The EasyFit commercial software was used to investigate the epistemic uncertainty. A number of about 60 statistical distributions used to fit the empirical distribution were ordered according to Kolmogorov-Smirnov, Anderson-Darling and Chi-Squared tests.

During statistical processing, it was found that the first 8-10 ranked distributions should be kept to define the lower and the upper limits of the epistemic uncertainty interval. That means that, for a given probability of exceedance $P\%$, the peak discharge $Q_{P\%}^{max}$ belongs to an interval denoted by $(Q_L^{max}, Q_U^{max})_{P\%}$ where the symbols L and U refer to the lower and the upper limit respectively of the uncertainty interval. Consequently, $Q_{P\%}^{max}$ results not being unique as usually accepted, but it has an infinite number of values for the same probability of exceedance $P\%$.

To avoid the arbitrary selection of the number of retained distributions, one has proceeded as follows:

The discharges $Q_{0.1\%}^{max}$ computed with the analysed statistical distributions are organized in descending order.

a) The lower and upper values of the interval of epistemic uncertainty, $(Q_L^{max})_{0.1\%}$ and $(Q_U^{max})_{0.1\%}$ respectively, are chosen according to a pre-defined percentage difference between these limits. For example, the difference between the selected upper and lower values should not exceed 20-25% in order to avoid a large interval of uncertainty:

$$\frac{(Q_U^{max})_{0.1\%} - (Q_L^{max})_{0.1\%}}{(Q_U^{max})_{0.1\%}} \leq 0.20 \ldots 0.25 \quad (2)$$

b) The distributions inside, but close to the interval limits $(Q_L^{max}, Q_U^{max})_{P\%}$ are then chosen as the lower and upper margins of the uncertainty interval.

An example of uncertainty interval for annual maximum discharges is presented in Figure 2. The presence of an outlier should be noted. The empirical probability for this discharge is about 2.4%, while the theoretical probability of the same value is in the range 0.5-1%.

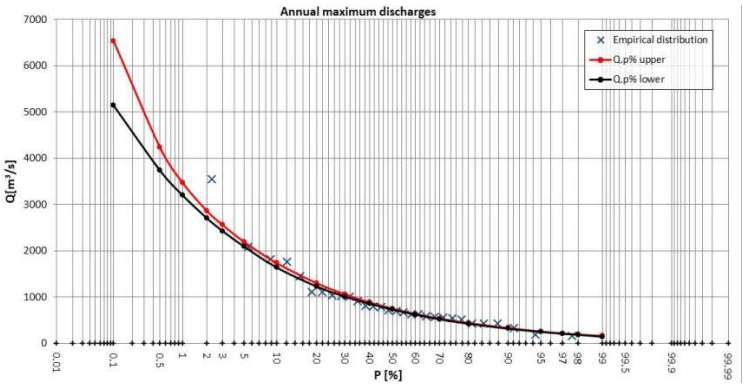

Figure 2. Uncertainty interval for the annual maximum discharges (Rădăuți-Prut gauge station).

2.2. Flood volumes

As previously mentioned, the partial series of the floods volume have been processed by using a POT approach. Different recommendations concerning the selection of the

Preprints (www.preprints.org) | NOT PEER-REVIEWED | Posted: 13 May 2021 doi:10.20944/preprints202102.0363.v2

threshold have been observed, namely: (i) be chosen low enough that at least one event is included, each year [9], (ii) be equal with 85% of all daily discharges, (iii) be close to long-term mean discharge or (iv) to include in average 4 maximum values, per year [53]. Other option involves (v) choosing the threshold as the discharge corresponding to the warning level, or to the bankfull discharge (the maximum discharge of the river without overflowing its banks). Usually, the bankfull discharge corresponds to a sharp change in the slope of the rating curve [63]. Finally, (vi) in the case of a dam regulating the river flow, the threshold can be considered equal to the discharge capacity of the bottom gates of the dam.

In this paper, a first threshold Q_{thr1} was chosen in such a way the total number n of selected floods is equal with the number N of years with daily or sub-daily discharges. Thus, the empirical exceedance probability associated to each measured value can be interpreted as an annual probability [9]. In a certain year, 2-3 or more floods can be selected, while in dry years no flood is retained for future analysis. If $n \neq N$, the theoretical probabilities, which corresponding to the new average duration, must be converted into annual probabilities of exceedance (Appendix 1).

In considering the threshold Q_{thr1}, all floods whose discharges exceed this value are selected. The maximum excess discharges are assumed to be independent with an arbitrary distribution [39]. However, the fulfilment of these basic assumptions has to be tested.

For the floods above Q_{thr1}, a second threshold $Q_{thr2} = a\, Q_{thr1}$, where $a < 0.9$, is introduced in order to derive the floods volume. The threshold Q_{thr2} is chosen in such a way to obtain distinct floods. Thus two consecutive floods have to be separated by at least three-times the average time to rise, while the discharge between two consecutive floods has to drop below the value of the two thirds of the smaller of the two peaks [64, 65]. The independence of two successive flood events is ensured if the minimum time span between the two flood peaks is at least 7 days [52], or if the interval between them is 5 days for catchments < 45000 km², 10 days for catchments between 45000 and 100000 km², 20 days for catchments > 100000 km² [66].

For a selected flood, the flood duration D corresponds to discharges $Q(t) > Q_{thr2}$. In this approach, the duration of the selected floods is variable. The volume of interest is given by the integral of the discharges higher than the threshold [16], unlike other papers where the volume is computed for a fixed duration, for example 7 days [51, 52].

The flood volumes over Q_{thr2} are statistically processed, resulting the *interval of uncertainty* for the volumes $V_{P\%}$, denoted by $(V_L, V_U)_{P\%}$. That means an infinite number of volumes $V_{P\%}$ may correspond to the probability of exceedance $P\%$ (Figure 3).

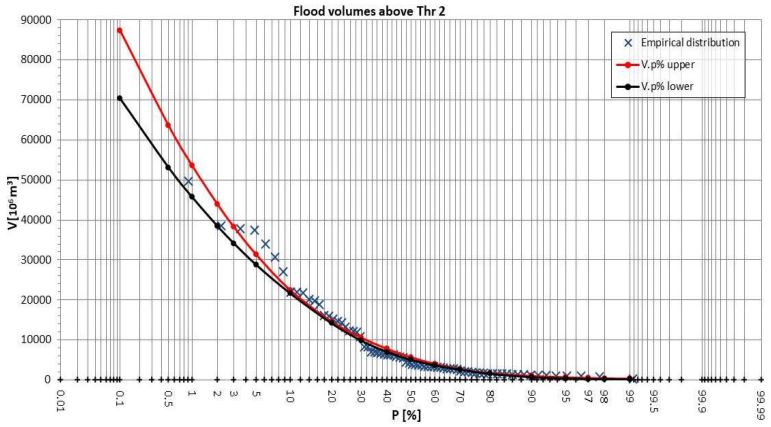

Figure 3. Uncertainty interval for the flood volume (Turnu-Măgurele gauge station).

2.3. Critical floods

The obtained two uncertainty intervals for the maximum discharge, respectively for the flood volume, define a space $((Q_L^{max}, Q_U^{max})_{P\%}$ x $(V_L, V_U)_{P\%})$ in which theoretically any point $(Q^{max}, V)_{P\%}$ belonging to it represents a possible solution. However, the DF,

Preprints (www.preprints.org) | NOT PEER-REVIEWED | Posted: 13 May 2021 doi:10.20944/preprints202102.0363.v2

cannot have simultaneously both the maximum discharge $Q_{P\%}^{max}$ and the volume $V_{P\%}$, where $Q_{P\%}^{max}$ and $V_{P\%}$ represent the best estimates of the univariate variables. This point belongs to a hydrograph whose PE is unknown, thus being defined by the common probability of the marginal probabilities of peak and volume [3]. High peak discharge does not necessarily mean high hydrograph volume [67] and vice-versa.

Considering the uncertainty for maximum discharges and flood volumes, one of the the most critical (yet plausible) combination for hazard estimation can be obtained by considering the upper limit of the maximum discharge as being coupled with the lower limit of the volume $(Q_{U,P\%}^{max},\ V_{L,P\%})$. This will be referred in this text as the *Maximum Design Flood (MDF).* Yet, no limitations are linked to this approach. Hence, the maximum discharge $Q_{U,P\%}^{max}$ can be combined with other volumes that belong to $(V_{L,P\%}, V_{U,P\%})$, thus obtaining a set of floods. The MDF is a necessary in establishing the dike's height, as well as the spillways dimensions, by considering the top level of the conservation storage at the spillway crest level.

Another critical flood is characterized by the upper limit of the flood volume coupled with the lower limit of the maximum discharge $(Q_{L,P\%}^{max},\ V_{U,P\%})$, which will be called *Maximum Volume Flood (MVF).* This flood is mainly used to establish the flood protection volume of the reservoir, both under the spillway crest level and above it in order to define the top of the storage reserved for flood control.

Both MDF and MVF should be used to decide on the framework operation rules of the reservoirs, during medium and extraordinary floods. At the same time, both types of floods represent boundary conditions for determining the position of the infiltration curve through dikes and for dike stability evaluations, during flood periods. Since the MDF has a lower duration than the MVF, while its maximum discharges are higher, it can lead to a potentially risky situation. At the same time, the MVF can also put the dike stability into danger (even if its maximum discharges are lower than in the case of MDF), because of its large duration. Finally, both types of floods can be used for deriving the uncertainty related to the delineation of the flooded areas as requested in the new cycle of implementation of the Flood Directive.

The selection of most critical floods is similar to that recommended by Volpi and Fiori [16] in a copula approach. In the same context, Prohaska and Ilić [22] have recommended the use of some 4 characteristic points, of which 3 points are located on the isoline $H(Q^{max}, V)_{P\%}$ corresponding to the probability of exceedance $P\%$ of the couple (Q^{max}, V). The 4th point - which characterizing the "maximum possible hydrograph" - is $(Q_{P\%}^{max}, V_{P\%})$, whose PE is still lower than $P\%$.

2.4. Shape of the design flood

For defining the hydrograph (and implicitly the shape) of the DF, its basic parameters (maximum discharge $Q_{P\%}^{max}$, flood volume V, duration D, time to peak T_{peak}) and its analytic expression (Figure 1) are to be established.

An alternative is to obtain a DF (or a family of DFs) that reproduces feasibly the shape of remarkable floods occurred in the past. This approach is more reliable, since it incorporates the specificity of the river basin.

In order to obtain the floods shape, all the floods above the threshold are to be normalized. They are scaled down on dimensionless abscissa and ordinate, the value of 100% corresponding to the flood duration, respectively to the maximum discharge of each flood.

The normalized floods have the same shape as the registered floods and are obtained as follows:

$$t_i = \frac{T_i - T_s}{D} \cdot 100 \quad [\%], \tag{3}$$

$$q_i = \frac{Q_i - Q_{thr2}}{Q_{max} - Q_{thr2}} \cdot 100 \quad [\%], \tag{4}$$

where:

Preprints (www.preprints.org) | NOT PEER-REVIEWED | Posted: 13 May 2021 doi:10.20944/preprints202102.0363.v2

t_i – time corresponding to discharge q_i of the dimensionless hydrograph [%];
T_i - time of recording discharge Q_i [dd/mm/yyyy hh:mm];
T_s - starting time of the recorded flood [dd/mm/yyyy hh:mm];
D - total duration above the threshold Q_{thr2} of the recorded flood [day];
q_i - discharge value of the dimensionless hydrograph [%];
Q_i - discharge at the moment T_i for the recorded hydrograph [m³/s];
Q_{thr2} – threshold for separating distinct floods [m³/s];
Q_{max} - maximum discharge (the peak) of the current flood [m³/s].

The normalized floods are grouped into classes that contain dimensionless floods with a similar shape, so that a set of up to 10-15 classes (depending on the duration with available data) is generated.

The floods are sorted out into the following categories: single peak, 2 peaks and multiple peaks. The normalised floods with a single peak can be subdivided according to the position of the peak: peak below 20%; peak in the range (20-30%); (30-40%); (40-60%) or above 60%. If necessary, the discretisation of the normalized time axis can be densified.

For each class, an average dimensionless hydrograph is obtained considering the dimensionless hydrographs weighted by the following factor:

$$w_f = \frac{Q_{\max(f)} - Q_{thr2}}{\sum_{j=1}^{n}(Q_{\max(j)} - Q_{thr2})} \quad (5)$$

where:

w_f – weighting factor for the dimensionless flood f [-];
$Q_{\max(f)}$ – peak discharge of the dimensionless flood f [m³/s];
n – number of dimensionless floods that belong to the same class [-].

As an example (Figure 4a), the average dimensionless flood of the Class 2 is the weighted average of dimensionless floods 58 and 67, where the weighting factors are: w_{58}= 0.31 and w_{67} = 0.69. The shape of the Class 9 is given by the weighted average of 8 floods (Figure 4b).

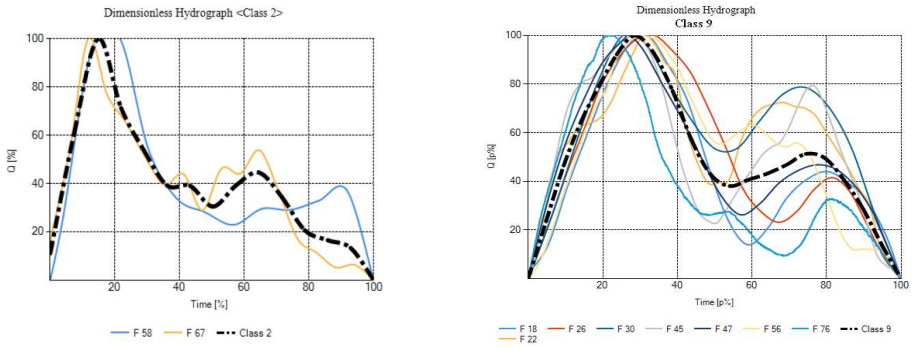

(a) **(b)**

Figure 4. Examples of average dimensionless floods: **(a)** Class 2; **(b)** Class 9

If a class contains only one flood, this very flood will determine the shape of that class.

2.5. Compactness coefficient of the Design Flood

To obtain the *compactness coefficient* of the DF, one should proceed as follows:

a) The first K significant floods are retained in the descending order of the maximum discharges. For the analysis of the most dangerous floods, $K \leq 5$ are recommended.
b) The selected floods, which based the deducted value of the threshold Q_{thr2}, are to be normalized.

Preprints (www.preprints.org) | NOT PEER-REVIEWED | Posted: 13 May 2021 doi:10.20944/preprints202102.0363.v2

c) The compactness coefficients $\gamma_{k=\overline{1,K}}$ of the dimensionless floods are computed taking into account that after normalization $q_{max} = 1$ and $t_{tot} = 1$:

$$\gamma = \frac{\sum_{i=2}^{n} \frac{q_{i-1} + q_i}{2} (t_i - t_{i-1})}{q_{max} \cdot t_{tot}} = \sum_{i=2}^{n} \frac{q_{i-1} + q_i}{2} (t_i - t_{i-1}), \quad (6)$$

d) **Maximum discharge flood.** The compactness coefficient of the first ranked out the above processed recorded floods is denoted by γ_d (the letter d represents discharge). As mentioned before, an average dimensionless flood is derived for each class. The compactness coefficient for MDF will be kept at the value γ_d for the set of all classes of shapes, while the time to peak will be different for each class (Figure 5).

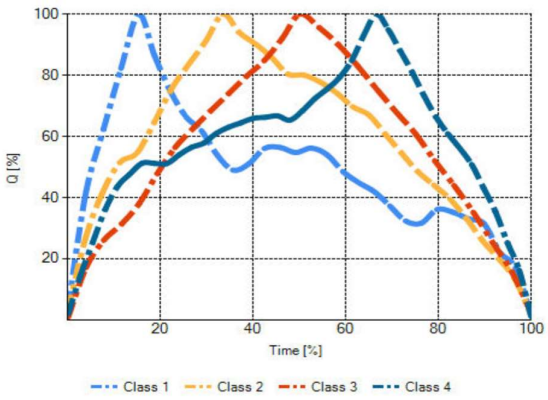

Figure 5. Set of average dimensionless floods.

Should one decide to provide a single flood to characterize the shape of the MDF, instead of a set, its shape will be similar to the shape of the first ranked of the recorded floods, sorted out in descending order of their maximum discharges. The dimensionless time to peak is denoted by t_{peak}^{d}. The current time value is t_i^d, while its corresponding discharge is q_i^d (the letter d of the exponent stands for discharge).
If the DF is defined analytically, the compactness coefficient is also kept at the value γ_d in all cases, irrespective a single shape or a set of shapes would be considered.

e) **Maximum volume flood**. As in the case of MDF, the first K dimensionless floods in the descending order of the maximum discharges are considered, and the maximum value of the compactness coefficient is chosen:

$$\gamma_v = \max_k \{\gamma_{k=\overline{1,K}}\}, \quad (7)$$

The letter v stands for volume. The current dimensionless time is t_i^v and its corresponding discharge is q_i^v. For the case with a set of shapes, the compactness coefficient of the averaged normalized floods for each class will be kept at the same value γ_v, while the time to peaks will be different for each class of the set.

If a single flood defines the shape of the MVF, its shape will be similar to the shape of the flood characterized by the compactness coefficient γ_v, with the time to peak t_{peak}^{v}.

Similar considerations can be made when the shape of the synthetic floods is given by analytical relations

2.6. Duration of the Design Flood

The duration $D_{P\%}$ of the Design Floods for the probability of exceedance $P\%$ is calculated with the relation:

Preprints (www.preprints.org) | NOT PEER-REVIEWED | Posted: 13 May 2021 doi:10.20944/preprints202102.0363.v2

$$D_{P\%}^{MDF} = \frac{(V_L)_{P\%}}{\gamma_d\left(Q_{U,P\%}^{max} - Q_{thr2}\right)}, \tag{8}$$

$$D_{P\%}^{MVF} = \frac{(V_U)_{P\%}}{\gamma_v\left(Q_{L,P\%}^{max} - Q_{thr2}\right)}, \tag{9}$$

where $D_{P\%}^{MDF}$ and $D_{P\%}^{MVF}$ are the duration of the MDF, and MVF, respectively. It was assumed the compactness coefficients γ_d and γ_v are constant, irrespective their probability of exceedance $P\%$.

The flood duration $D_{P\%}$ varies with $P\%$. For the same PE, the duration $D_{P\%}$ is shorter for the MDF as compared to the MVF.

2.7. Time to peak of the Design Flood

The time to peak of the DF is:

$$\left(T_{peak}\right)_{P\%} = t_{peak} \cdot D_{P\%}, \tag{10}$$

where - for the case of single design floods - t_{peak} is to be replaced by t_{peak}^{d} for the MDF and by t_{peak}^{v} for the MVF. The computed values for $\left(T_{peak}\right)_{P\%}$ are different for MDF and MVF respectively.

In the case of a set of DFs, the time to peak in each class is computed with a similar relation, $D_{P\%}$ being kept at the same value, irrespective of the class.

2.8. Construction of Design Floods

To obtain the ordinates of the DFs which corresponding to the probability of exceedance $P\%$, the normalized ordinates q_i of the MDF and MVF are multiplied with the maximum discharge (from which the threshold Q_{thr2} had been extracted), and further the threshold value Q_{thr2} is added to the ordinates thus obtained. The time values on the abscissa are obtained by multiplying the dimensionless time with the flood duration.

Thus, for the MDF, the following can be written:

$$(Q_i^{MDF})_{P\%} = q_i^d \cdot \left((Q_U^{max})_{P\%} - Q_{thr2}\right) + Q_{thr2} \tag{11}$$

$$(T_i^{MDF})_{P\%} = t_i^d \cdot D_{P\%}^{MDF}. \tag{12}$$

For the MVF, the coordinates of the DF are:

$$(Q_i^{MVF})_{P\%} = q_i^v \cdot \left((Q_L^{max})_{P\%} - Q_{thr2}\right) + Q_{thr2}, \tag{13}$$

$$(T_i^{MVF})_{P\%} = t_i^v \cdot D_{P\%}^{MVF}. \tag{14}$$

An ensemble of Synthetic or DFs is presented in Figure 6.

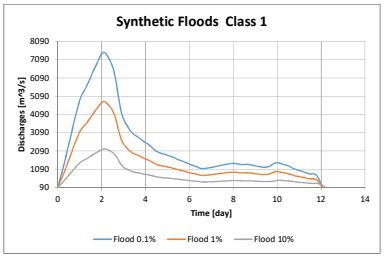

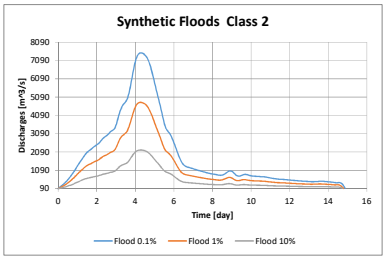

Preprints (www.preprints.org) | NOT PEER-REVIEWED | Posted: 13 May 2021 doi:10.20944/preprints202102.0363.v2

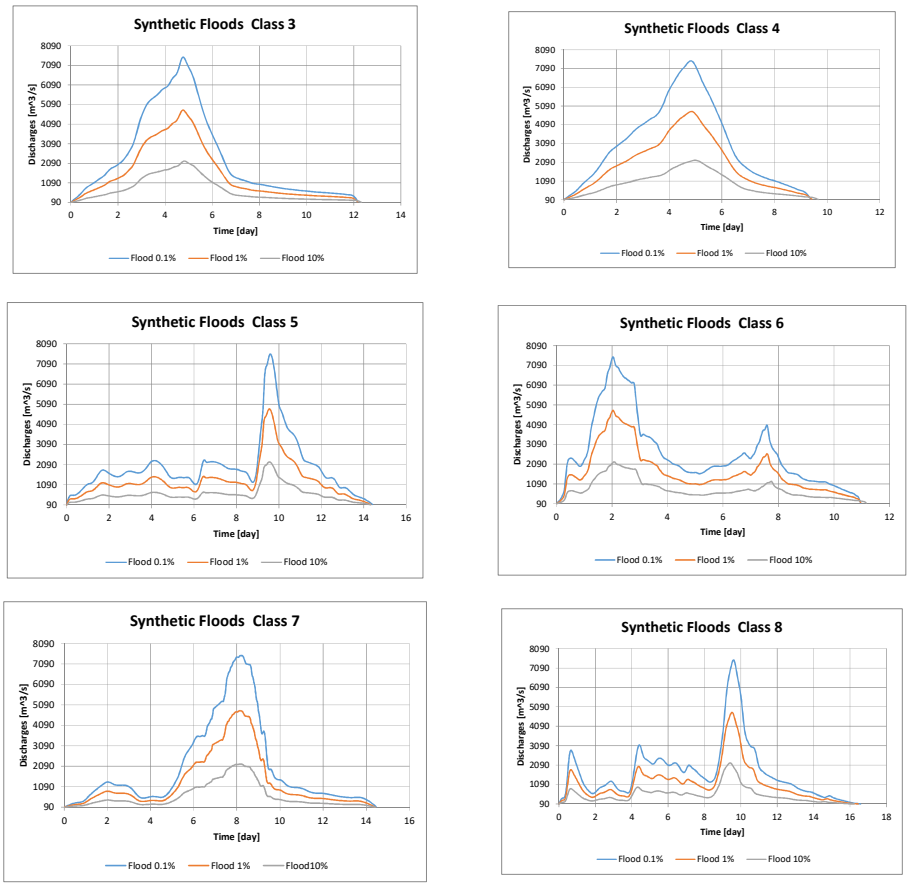

Figure 6. Sets of design floods (Rădăuți-Prut gauge station).

3. Case studies

In the following, two case studies will be presented. The first case study was analysed in the frame of Danube Floodrisk project (DANUBE FLOODRISK - PA 05 (danube-region.eu) [68] SEE (South East Europe) transnational and interregional programme, while the second case study was undertaken to support EastAvert project in the frame of the Joint Operational Programme Romania-Ukraine-Republic of Moldova [69].

In both cases, the data for the Romanian territory have been provided by the National Institute of Hydrology and Water Management (NIHWM), Bucharest, Romania.

3.1. Case study no. 1

The Danube River and its tributaries have been the object of numerous initiatives for European cooperation, like The International Commission for the Protection of the Danube River (ICPDR/ created in 1998) that promotes policy agreements for improving the condition of the Danube and its tributaries, or the EU Strategy for the Danube Region (EUSDR) as endorsed by the European Council in 2011.

An important scientific research work [54] was completed in 2019 by scientists from 11 countries of the Danube River Basin. The work was performed and carried out with the involvement of the National Committees of IHP UNESCO of the Regional cooperation of the countries in the Danube River Basin under the coordination of the Institute of Hydrology of the Slovak Academy of Sciences. One of the Romanian river locations on the Lower Danube, which were involved in this study was the Turnu Măgurele gauge station.

Preprints (www.preprints.org) | NOT PEER-REVIEWED | Posted: 13 May 2021 doi:10.20944/preprints202102.0363.v2

The complete time series of maximum daily discharges registered at this station from 1931 to 2008 was available for the statistical analysis.

The time series had been checked for potential trends, with conclusion that the stationarity assumption would be justifiable. The results of the statistical tests concerning the mutual independence and identical distribution, the homogeneity and the lack of trend of the annual maximum discharges are presented in Table 1.

Table 1. Results of the statistical tests.

Statistical Test	Statistics	|Z| statistics	Z quantile	First degree error	Conclusions
Wald-Wolfowitz	R=31	1.74264	$Z_{0.05} = 1.65$ $Z_{0.025} = 1.96$	0.0814	Mutual independence 5% threshold
Turning point	T=50	0.18115	$Z_{0.05} = 1.65$	0.85626	i.i.d 10% threshold
Mann-Whitney-Wilcoxon	W=700	0.03179	$Z_{0.05} = 1.65$	0.97464	Mutual Homogeneity 10% threshold
Mann-Kendall	T=-115	0.49192	$Z_{0.05} = 1.65$	0.62278	No trend 10% threshold

According to the statistical tests, in all cases the null hypothesis (mutual independence, mutual homogeneity and lack of trend) was accepted with a threshold 10%. The only exception was the Wald-Wolfowitz test, where the null hypothesis was accepted for 5% threshold, while still being discarded for the 10% threshold.

The explanation for the lack of trend of the annual maximum discharges is related to the sizable extension of the Danube river basin, which is able to compensate at least in the lower Danube the local effects of the climate changes. Thus, one can feasibly consider that the variation of the maximum discharges for the lower Danube is due mainly to natural variability.

3.1.1. Maximum discharges

A significant number of probability distributions have been used to define the uncertainty interval [68, 70]. The obtained results – as keeping the first 9 ranked distributions, according to Kolmogorov-Smirnov test - are presented in Table 2.

Table 2. Maximum discharges on Lower Danube, at Turnu-Măgurele gauge station.

P%	POT (m^3/s)		POT* (m^3/s)		AMS (m^3/s)	
	Q lower	Q upper	Q lower	Q upper	Q lower	Q upper
0.1	8321	11346	16621	19646	17317	19884
1	7453	8238	15753	16538	15825	16888
10	5133	5450	13433	13750	13541	13679

* Values from statistical processing to which the selected threshold value (Q_{thr2} = 8300 m^3/s) was added.

According to Table 2, the uncertainty interval for 1% annual probability of exceedance (AMS) is in the range (15825 -16888) m^3/s. The maximum discharge - as recorded at Turnu Măgurele on 23-24 April, during the 2006 flood - was 16300 m^3/s and according to NIHWM that value corresponded to $P\%$ =1%. It is herein noted that this discharge fits perfectly between the limits of the uncertainty interval

3.1.2. Flood volumes

For the separation of the significant floods, the daily discharges between 1931-2008 were analysed. The threshold values for floods selection were Q_{thr1} = 9700 m^3/s, while

Preprints (www.preprints.org) | NOT PEER-REVIEWED | Posted: 13 May 2021 doi:10.20944/preprints202102.0363.v2

Q_{thr2} = 8300 m³/s. All discharges greater than 8300 m³/s were taken into consideration for computing the flood volume.

The uncertainty limits of the volumes are presented in Table 3.

Table 3. Flood volumes above Q_{thr2} at Turnu-Măgurele gauge station

P%	V lower (10^6 m³)	V upper (10^6 m³)
0.1	70384	87390
1	45768	53677
10	21633	22428

3.1.3. Flood shape

In the Table 4 herebelow, the first 5 floods in decreasing order of the maximum discharge, as well as their defining parameters (maximum discharge, total volume, volume above the threshold Q_{thr2}, compactness coefficient, time to peak and flood duration) are presented.

Table 4. Floods at Turnu-Măgurele gauge station and their parameters.

Flood number	Starting date	Maximum discharge (m³/s)	Flood volume (10^6 m³)	Volume above Q_{thr2} (10^6 m³)	Compactness coefficient (-)	Time to peak (days)	Flood duration (days)
80	07/03/2006	**16300**	94198	31880	**0.53**	45.9	86.9
38	14/02/1970	14940	161521	49641	0.55	106.3	156.0
31	13/03/1962	14700	78827	21642	0.49	40.7	79.7
55	12/03/1981	**14400**	45298	14292	**0.63**	17.2	43.2
54	30/04/1980	14400	47509	12370	0.48	26.0	49.0

By taking into consideration the maximum discharge and the compactness coefficient, only the floods that occurred in 2006 and 1981 were considered for the next steps. The MDF (Class 1) and MVF(Class 2) are presented (Figure 7; Tables 5 and 6).

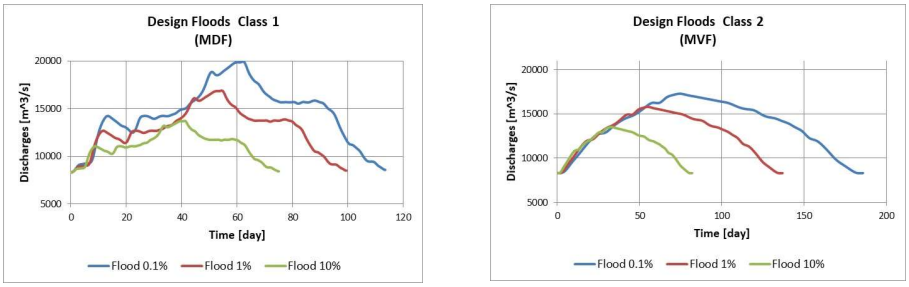

(**a**) (**b**)

Figure 7. Design Floods: **(a)** MDF for Class 1 and **(b)** MVF for Class 2

Table 5. Main parameters of MDF Class 1 at Turnu-Măgurele gauge station

P%	Q upper (m3/s)	V lower above threshold (10^6 m³)	Total V lower (10^6 m³)	Flood duration above threshold (days)
0.1	19884	60145	141508	116
1	16888	39108	110432	100*
10	13679	18485	72359	75

* In 2006 the maximum discharge at Turnu-Măgurele gauge station was 16300 m3/s, the flood volume above the threshold (8300 m³/s) was 31880 mil. m³ and the flood duration above the threshold was 87 days.

Preprints (www.preprints.org) | NOT PEER-REVIEWED | Posted: 13 May 2021 doi:10.20944/preprints202102.0363.v2

Table 6. Main parameters of MVF Class 2 at Turnu-Măgurele

P%	Q lower (m3/s)	V upper above threshold (10^6 m^3)	Total V upper (10^6 m^3)	Flood duration above threshold (days)
0.1	17317	87390	220534	185
1	15835	53677	151682	137*
10	13541	22428	81231	82

* In 1970 the maximum discharge at Turnu-Măgurele gauge station was 14940 m^3/s, the flood volume above the threshold (8300 m^3/s) was 49641 mil. m^3, and the flood duration above the threshold was 156 days.

3.2. Case study no. 2

The Rădăuți-Prut gauge station is located on Prut River, about 125 km upstream Stânca-Costești reservoir. It is not influenced by the backwater effect, even at exceptional water levels in the reservoir. The catchment area by the dam section is 12,000 km^2. Among the 247 large dams in Romania, the Stânca-Costești dam is ranked the second after the Iron Gates Dam on Danube in terms of reservoir volume, having the total capacity 1,285 mil.m^3. The surface area of the reservoir is 77 km^2, while its length - at the maximum water level, during floods - is about 120 km. The flood control storage, between the top of the conservation level and the top of the surcharge pool (the maximum allowed water level in the reservoir, during extraordinary floods corresponding to 0.1% probability of exceedance of the maximum discharge), is 665 mil.m^3.

Two major floods did occur in the first decade of this 21st century, namely: the first, between 25 July - 02 August 2008, which was characterized by a very compact shape, with a maximum discharge of 3552 m^3/s and a volume of about $1.16 \cdot 10^9$ m^3 (Figure 8a), while the second one, in 2010, had the maximum discharge of 2080 m^3/s, a very large duration and an exceptional volume of $2.45 \cdot 10^9$ m^3 (Figure 8b). The comparison of the volumes of each of the 2 floods with the reservoir volume assigned to flood control (665 $\cdot 10^6$ m^3) puts into evidence the rather critical attenuation process - with still safe conditions - that took place then at Stanca-Costesti.

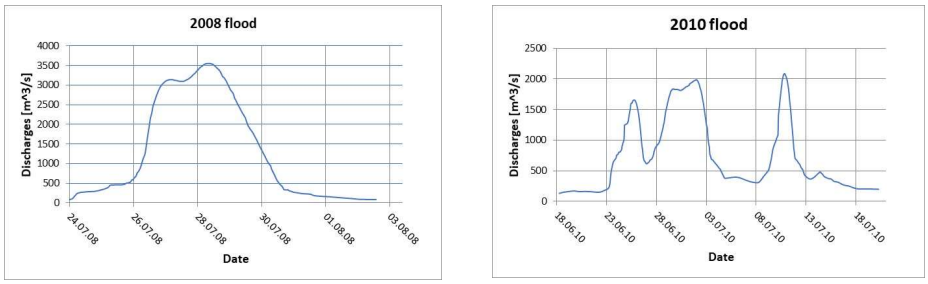

(a) **(b)**

Figure 8. Extraordinary floods recorded in 2008 and 2010 respectively: **(a)** 2008; **(b)** 2010.

From a hydrological point of view, the flood of 2010 had 2 peaks, being followed after 5 days by another flood. However, from the point of view of flood management, the 2 floods have constituted an only flood event, the second flood occurring in the conditions of already very high water levels in the reservoir. Consequently, to define the design flood, the hydrological system of the 2 floods was considered.

Considering the decreasing order of the maximum discharges and flood volumes series, the maximum discharge of 2008 was 40% higher than the following peak, while the flood volume of 2010 was 2 times higher than the next flood volume. They both represent outliers of their time series.

Preprints (www.preprints.org) | NOT PEER-REVIEWED | Posted: 13 May 2021 doi:10.20944/preprints202102.0363.v2

A critical situation in the reservoir operation occurred in 2008, under the conditions of a very compact flood, while the spillways were being used at their maximum discharge capacity in order to prevent overflowing of the dam. Water level in the reservoir reached 98.27 m.a.s.l. overpassing the upper limit of the flap gates (98.20 m.a.s.l.), which corresponded to the design flood level for medium floods (1% probability of exceedance of the maximum discharge).

Since the Stânca-Costești reservoir was put into operation in 1978, the occurring flood characteristics modified, thus requiring a re-evaluation of the maximum discharges and flood volumes and the subsequent change in the operation rules of the reservoir, during medium and extraordinary floods.

An update of the maximum discharges in 2007 and in 2018 respectively is provided in the Table 7.

Table 7. Maximum discharges at Rădăuți-Prut

P%	Evaluation 2007	Re-evaluation 2018	
	Pearson 3	LogN 3p	LogN 2p
0.1	4300	5143	5425
1	2800	3203	3311
10	1500	1670	1686

Compared with the 2007-evaluation, one can notice an increase of maximum discharges of about 16% for $P\% = 0.01\%$ and some 12.5% for $P\% = 1\%$.

According to the herein presented methodology, the floods above the threshold 2 (which was set to 90 m3/s representing the average discharge) were normalised and then grouped into classes of similar shape. Hence, the flood of class 9 had reproduced the shape of 2008 flood, while the flood of class 10 had a similar shape to 2010 flood.

In following the statistical processing of the maximum discharges and flood volumes, the design floods were derived. Only the design floods for classes 9 and 10 are presented due to the exceptional character of these floods. (Table-8 and Figure-9).

Table 8. Parameters of the design floods at Rădăuți-Prut

$P\%$	Flood type	$Q_{P\%}^{max}$ (m^3/s)	$V_{P\%}$ (10^6 m^3)	Class 9		Class 10	
				T_{peak} (days)	D (days)	T_{peak} (days)	D (days)
0.1%	MDF	6543	2760	7.5	13.5	6.6	13.5
	MVF	5145	3598	11.0	20.0	9.3	21.8
1%	MDF	3476	1713	8.0	16.2	7.1	15.2
	MVF	3204	2020	9.4	20.2	8.5	17.3
10%	MDF	1738	719	6.7	13.2	5.2	12.3
	MVF	1641	743	7.4	14.7	5.7	12.8

Preprints (www.preprints.org) | NOT PEER-REVIEWED | Posted: 13 May 2021 doi:10.20944/preprints202102.0363.v2

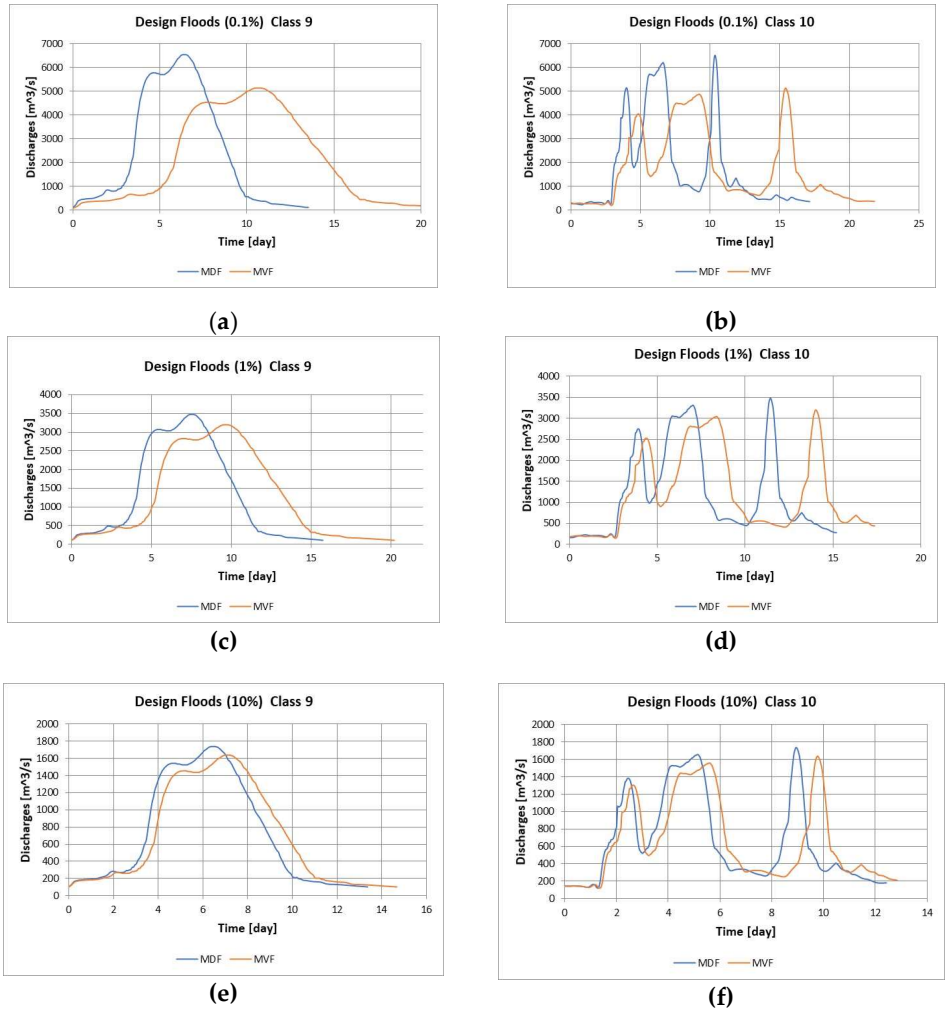

Legend: MDF – blue solid line; MVF – orange solid line

Figure 9. Maximum discharge flood and maximum volume flood
(a), (c), (e) Class 9. **(b), (d), (f)** Class 10. **(a)** and **(b)** Q 0.1%; **(c)** and **(d)** Q 1%; **(e)** and **(f)** Q 10%.

Figure 9 shows the MDF and MVF of the classes 9 (left side) and 10 (right side) for $P\% = 0.1\%$; 1% and 10% respectively. For a given PE, the classes 9 (1 peak flood) and 10 (3 peaks flood) have different shapes, but the maximum discharge and the flood volume respectively are the same. For example, for both classes at 0.1% the MDF is characterized by $Q_{P\%}^{max} = 6543$ m³/s and $V_{P\%} = 2760 \cdot 10^6$ m³, while in the case of MVF $Q_{P\%}^{max} = 5145$ m³/s and $V_{P\%} = 3598 \cdot 10^6$ m³.

It can also be seen that, for the same class, the differences between MDF and MVF diminish as $P\%$ increases (ex.Figure 9 (a), (c), (e)).

4. Discussion

1. The limits of the *uncertainty interval* can be established in different ways, namely:

(i) By selecting a large number of statistical distributions, such as presented in the previous chapters. The basic idea is to define *upper* and *lower limits* of the uncertainty intervals and further obtain the MDF and MVF by establishing the appropriate combinations for the pairs $(Q_U^{max}, V_L)_{P\%}$ and $(Q_L^{max}, V_U)_{P\%}$ respectively;

Preprints (www.preprints.org) | NOT PEER-REVIEWED | Posted: 13 May 2021 doi:10.20944/preprints202102.0363.v2

(ii) By choosing the *best distribution*, as based on statistical tests and using the confidence interval to define the lower and the upper limits of the maximum discharges and flood volumes respectively. The recommended confidence level β is 90-95% [52], but it can be reduced to avoid a large difference between the upper and lower limit of the uncertainty interval;

(iii) As based on the uncertainty analysis of bivariate design flood [52]. For a given PE the contour lines (AND copula) of the upper and lower bounds of the interval of uncertainty put into evidence an infinite number of hydrograph coupled characteristics (maximum discharge, flood volume), which approximately satisfy the condition:

$$H(Q^{max}, V)_{P\%} \cong P(Q^{max} \geq Q_{P\%}^{max};\ V \geq V_{P\%}) \quad (15)$$

In this paper, the lower and the upper limits of the uncertainty interval for copula were obtained by using the distributions that led to the uncertainty interval for univariates. For bivariates, the Gumbel-Hougaard copula perform the best for modeling the joint distribution of peak discharges and flood volume [28, 52, 67].

The main parameters (maximum discharge and flood volume) which characterize the MDF and MVF are located quite close to the upper limit of Gumbel-Hougaard (G-H) uncertainty interval (Figure 10). (Notice is still made that the resulted differences are not very concerning. For instance, $Q_{1\%}^{max} = 3320$ m³/s, while $Q_{U,1\%}^{max} = 3476$ m³/s).

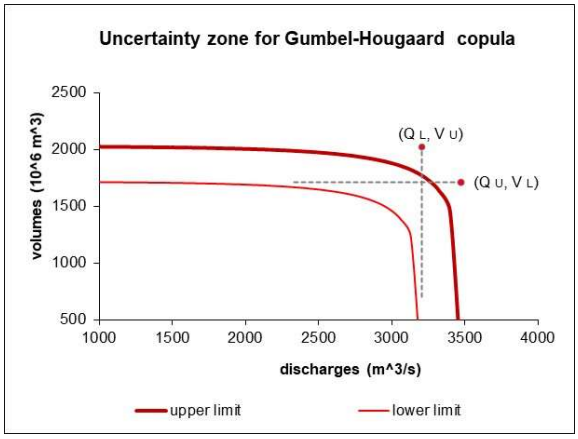

Figure 10. Uncertainty zone $P\%$=1% (Rădăuți-Prut gauge station).

2. The simulations of the reservoir operation considering a set of floods of the same PE put into evidence the most critical situations associated with the operation of the dam outlets. These do likely occur during floods having significant compactness coefficients. A high gradient of incoming water volumes into the reservoir means a large volume of water should be outflown from same reservoir in a short period of time, in order to avoid created critical levels in the reservoir. Yet, at the same time, the outflowing discharges must not exceed, as far as possible, the carrying capacity of the downstream riverbed.

3. The DF for $P\% = 0.1\%$ on the Lower Danube at Turnu-Măgurele gauge station (Figure 11) had a total duration - over the threshold (Q_{thr2} = 8300 m³/s) - between 116 days (MDF) and 185 days (MVF). This duration was plausible taking into account that 1970 flood duration, which had the largest volume registered in 78 years, was 157 days.

Preprints (www.preprints.org) | NOT PEER-REVIEWED | Posted: 13 May 2021 doi:10.20944/preprints202102.0363.v2

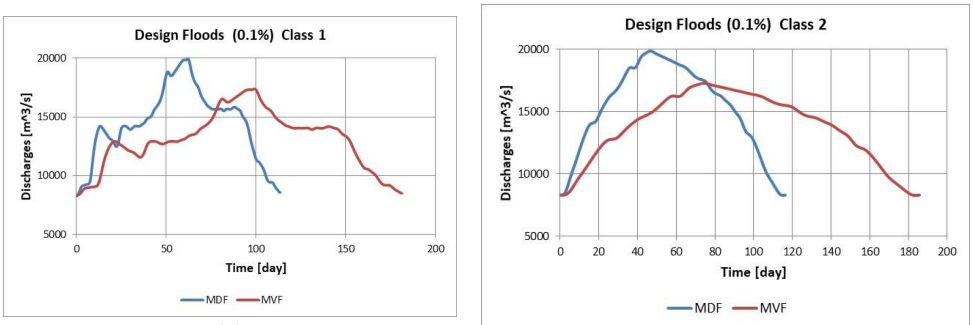

Figure 11. MDF and MVF: **(a)** Class 1; **(b)** Class 2.

4. The DFs that reproduce the shape of recorded floods are likely more reliable than the analytic floods (Figure 1). If the DF that reproduces the shape of the recorded floods for classes 9 and 10 at Rădăuți-Prut station overlaps with the analytic flood characterized by the same parameters, it is found that there is a fairly good agreement in the case of unimodal floods (Figure 12 a), yet quite important differences do occur for multimodal floods (Figure 12 b).

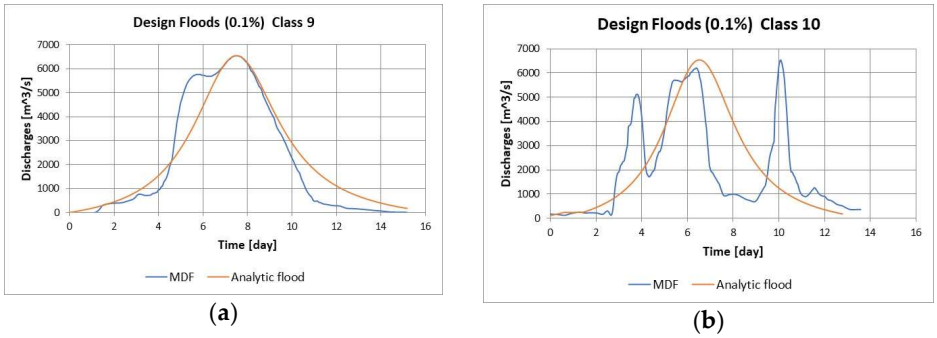

Figure 12. Overlapping MDFs (analytic expression and recorded shape)

5. If the analysis purpose is to delineate the flooding areas, the analytic floods will lead to approximately the same results as the floods reflecting the shape of the recorded floods. If the purpose is to determine the framework rules for the optimal attenuation in a reservoir during flood conditions, it is preferable to use the shape of real floods especially in case of multi-peak floods.

5. Conclusions

The hydrological processing of flood waves can be performed at different degrees of complexity, depending on the future utilization of the results. The simplest way - as used in case of a rough spatial delineation of the flooded areas or for dikes deterministic design - is based on a river steady flow simulation, considering the maximum discharge corresponding to the probability of exceedance $P\%$. The discharge $Q_{P\%}^{max}$ is treated as a deterministic value, neglecting the associated uncertainty. In such a case, for each $P\%$ a unique extension of the flooded area is obtained.

The problem gains in complexity when hydrologic uncertainty is taken into account and more distributions are used to fit the recorded discharges. All of them approximate well the frequent values of the maximum discharges, but define a range of uncertainty for measured maximum discharges and extrapolated values. While the choice of the upper (U) and the lower (L) limits of this interval requires an expert judgement, yet normally, the difference between the minimum and maximum values for $P\% = 0.1\%$ should not

 doi:10.20944/preprints202102.0363.v2

exceed 20-25%. Based on the border values of the uncertainty interval for univariates, the main parameters $(Q_U^{max},\ V_L)_{P\%}$ for MDF and $(Q_L^{max},\ V_U)_{P\%}$ for MVF are defined for each probability of exceedance $P\%$. As such, the points $(Q_U^{max},\ V_L)_{P\%}$ and $(Q_L^{max},\ V_U)_{P\%}$ are located quite close to the outer contour line of the copula uncertainty interval for the same probability of exceedance $P\%$..

Apart from DF's key parameters (maximum discharge, flood volume), the shape of the DF hydrograph is equally important. The easiest way to establish the flood shape is to use an analytical curve that passes through the characteristic points of the flood hydrograph: (0, 0), $(T_{peak}\ , Q_{P\%}^{max})$, $(D\ , 0)$, while respecting the constraint of preserving the flood volume. Another methodological option (developed actually in this paper) is to generate a set of synthetic design floods that reproduce shapes of recorded floods, each DF being characterized - for a given $P\%$ – by the same parameters (maximum discharge, volume, duration).

The unimodal DFs have also been addressed by other researchers. Mediero et al [3] obtained a set of synthetic hydrographs that preserved the statistical characteristics of the observed peaks, while Volpi and Fiori [16] adopted an ensemble approach, by choosing the most critical events, in term of hydrological loads on the hydraulic structures.

The DFs set obtained with the proposed methodology can be reliably used for flood risk management or to examine riverane environmental consequences, associated with occurring floods. Yet, the most critical situations occur for compact floods, both for MDF and MVF. Mainly, the MDF can be used for the design of spillways, as well as for the dike design in order to foresee flooding high levels that would threat dike overtopping, while the MVF can be used for establishing the flood protection reserved volumes in reservoirs.

For the dike stability, both the MDF and MVF can be used. Although in case of MDF the high levels would last for short durations, the water pressure can still activate preferential routes of water seepage through the galleries created by rodents, endangering the stability of the dike. On the other hand, the long duration of MVF floods also makes them dangerous because of sustaining seepage curves which can ultimately spring at the downstream face of the dikes. Both types of DFs can be taken as boundary conditions for the non-permanent seepage of river waters through the dike and its foundation. The critical gradients will then be computed, putting into evidence the sensitive parts of the respective hydraulic structures

The Turnu-Măgurele daily discharges on Lower Danube were processed for deriving the MDF and MVF with the practical purpose of studying the stability of the dikes, the flood attenuation in floodplaine and the delineation of the flooded areas in case of dike breach.

Based on the Rădăuți-Prut discharges on Prut River, floods of different shapes were obtained in order to derive their influence on the optimal operation rules of the spillways and bottom gates of Stânca-Costești reservoir, for the case of medium and extraordinary floods.

It is largeley accepted that a single 'best estimate' of flood probabilities is not able to capture the epistemic uncertainty [71]. The solution proposed in this paper is to capture the uncertainties in the form of a set of design floods.

A future direction of this research, especially for medium or small river basins, is to consider the time dependency of the distribution parameters [43, 72], in order to derive the worst possible flood for a given PE.

Author Contributions: Conceptualization, R.D. and A.F.D.; methodology, R.D. and A.F.D.; software, A.F.D., D.C. and R.T.; validation, R.D., A.F.D., D.C. and R.T.; formal analysis, D.C., R.T.; investigation, R.D. and A.F.D.; data curation, A.F.D.; writing—original draft preparation, R.D.; writing—review and editing, R.D., A.F.D., D.C. and R.T.; visualization, A.F.D.; supervision, R.D.; project administration, R.D.; funding acquisition, R.D. All authors have read and agreed to the published version of the manuscript.

Funding: The elaboration of the Methodology was financed by the Romanian Government through the Ministry of Regional Development within the contract: Establishing the maximum flows and

Preprints (www.preprints.org) | NOT PEER-REVIEWED | Posted: 13 May 2021 doi:10.20944/preprints202102.0363.v2

volumes for the calculation of the hydrotechnical retention constructions. Revision of STAS 4068-1 / 82 and 4068-1.2 / 87. Subsequently, it was applied within the European funded projects Danube Floodrisk and EastEvert.

Acknowledgments: The authors are grateful to the National Institute of Hydrology and Water Management, Bucharest, Romania, for providing the data necessary for the study.

The authors are indebted to dr.ir. Constantin Stere (Dutch International Expert/ Rtd.Royal Haskoning, NL) for his pertinent revision on the English version of this paper.

Conflicts of Interest: The authors declare no conflict of interest. The funders played no role in the concept of this study; in the collection, analyses or the interpretation of data; in writing of the manuscript, or in the decision to publish the results.

Appendix A

If the number n of selected floods is different than the number N of the years with daily or sub-daily discharges ($n \neq N$), the average duration of the sampling interval d is less or greater than one year depending on more or fewer floods respectively than the number of years are selected. The theoretical probabilities of exceedance $P_d = P(d)$ - which corresponding to the maximum discharges over a period d, other than the year - must be converted into annual probabilities of exceedance $P_a = P_1 = P(1)$, which correspond to the same maximum discharges (Figure A1).

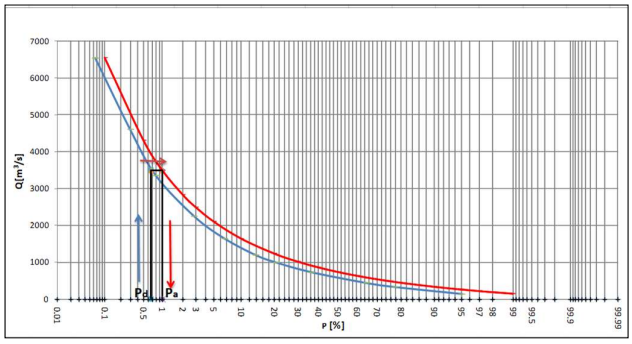

(a)

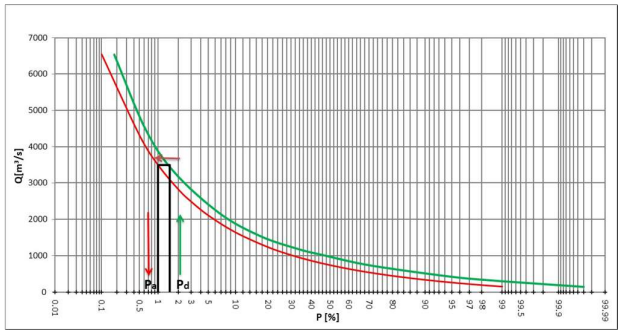

(b)

Legend: P_a = red line; P_d for $n > N$ = blue line; P_d for $n < N$ = green line.

Figure A1. The relationship between the probability of exceedance P_d % for the sampling interval d and the annual probability of exceedance P_a %: **(a)** $n > N$; **(b)** $n < N$.

If one denotes the annual PE with F_1^c (the index c indicates the complementary function of the cumulative distribution function), respectively by F_d^c the PE corresponding to an interval d different from one year, it can be stated that:

Preprints (www.preprints.org) | NOT PEER-REVIEWED | Posted: 13 May 2021 doi:10.20944/preprints202102.0363.v2

$$P_d = F_d^c(Q) \tag{A1}$$

hence it it results:

$$Q = (F_d^c)^{-1}(P_d) \tag{A2}$$

Therefore, the annual PE corresponding to the same flow rate Q is:

$$P_1 = F_1^c(Q) = F_1^c[(F_d^c)^{-1}(P_d)] \tag{A3}$$

A similar relationship is obtained if working with the cumulative distribution function (the probability of non-exceedance) instead of the exceedance probability:

$$P_1 = F_1(Q) = F_1[F_d^{-1}(P_d)] \tag{A4}$$

However, the calculation of the annual PE in this way encounters some difficulties, because many of the usual distributions do not admit the inverse; yet, the numerical inversion can be used if necessary.

An approximate solution can be obtained relatively easily, starting from the relation [35]:

$$P_N = 1 - (1 - P_1)^N \tag{A5}$$

where: P_1 is the annual PE of the discharge $Q_{P\%}^{max}$, and P_N is the PE of the same event for a period of N years.

Suppose that in N years with available data, a number of n floods above the threshold were selected, where n is greater than the number of years ($n>N$). In this case, the PE of the same event for a period of n intervals of average duration $d = N/n$ (years) is:

$$P_M = 1 - (1 - P_d)^n \tag{A6}$$

As shown before, for the same calculated discharge the probability of exceedance P_d must be put in correspondence with the annual probability of exceedance $P = P_1$, where d is the size of the average sampling interval expressed in years. Let be:

$$\begin{aligned} Q_N &= Q(P_N) \\ Q_n &= Q(P_n), \end{aligned} \tag{A7}$$

Equating the values of the two discharges is obtained:

$$Q(P_N) = Q(P_n), \tag{A8}$$

Applying the inverse function results:

$$Q^{-1}Q(P_N) = Q^{-1}Q(P_n), \tag{A9}$$

or:

$$P_N = P_n, \tag{A10}$$

It follows from here:

$$1 - (1 - P_1)^N = 1 - (1 - P_d)^n, \tag{A11}$$

The previous relation allows for the calculation of the exceedance probability corresponding to the new average time interval $d = N/n$ years as a function of the annual probability of exceedance:

$$P_{d=N/n} = 1 - (1 - P_1)^{N/n};\ n > N \tag{A12}$$

where P_1 is the annual PE (corresponding to a period of 1 year), and $P_{d=N/n}$ is the PE of the new interval.

Let be for example N = 85 years and n = 130 selected floods. According to the above formula, to obtain the discharge with an annual probability of exceedance 1%, the discharge corresponding to the probability of exceedance 0.65% based on the 130 selected values must be calculated.

If the number of n selected floods is less than the number of years N (i. e. $n < N$), the relation for the calculation of the probability of exceedance corresponding to a time interval $d = N/n$ years is similar to the previous one, but the average duration is now $d = N/n$:

$$P_{d=N/n} = 1 - (1 - P_1)^{N/n};\ n < N \quad \text{(A33)}$$

where P_1 is the annual PE (over a time interval of 1 year), and $P_{d=N/n}$ is the PE of the new average time interval, greater than one year. Let for example consider N = 85 years and n = 48 floods selected. To obtain the discharge with an annual probability of exceedance 1%, the discharge corresponding to the probability of exceedance 1.76% based on 48 selected values must be calculated.

The previous relationships allow for the transformation of probabilities P_d into annual probabilities of exceedance. However, these additional computations are not necessary if the number of selected floods is equal to the number of years with measured values.

References

1. Lo, S. *Glossary of Hydrology*. Water Resources Publications. Colorado, USA. 1992; pp.346-347.
2. Xiao, Y., Guo, S., Liu, P., Yan, B., Chen, L. Design flood hydrograph based on multicharacteristic synthesis index method, *J. Hydrol. Eng.* **2009**, 14(12), 1359–1364.
3. Mediero, L., Jimenez-Alvarez, A., Garrote, L. Design flood hydrographs from the relationship between flood peak and volume, *Hydrol. Earth Syst. Sci*. **2010**, 14, 2495– 2505.
4. Directive 2007/60/EC of the European Parliament and of the Council of 23 October 2007 on the assessment and management of flood risks.
5. Stedinger J.R., Vogel, R.M., Foufoula-Georgiou, E. Frequency Analysis of Extreme Events. In: *Handbook of Hydrology.* D. R. Maidment, Ed., McGraw-Hill, New York, USA., 1993; pp.18.1-18.66.
6. Pilgrim, D.H., McDermott, G.E., Mittelstadt, G.E. The rational Method for Flood Design for Small Rural Basins. In: *Catchment runoff and Rational Formula.* Yen, B.C. Editor. Water Resources Publications. Littleton, Colorado. USA. 1992; pp. 16-26
7. Smithers, J.C. Methods for design flood estimation in South Africa. *African Journals Online, Water, SA*. **2012.** Vol. 38 No. 4, pages 633-646, ISSN:0378-4738, DOI: 10.4314/wsa.v38i4.19
8. Yevjevich, V. *Probability and Statistics in Hydrology*. Water Resources Publications. Colorado, USA. 1972; pp.118-168.
9. Kitte, G.W. *Frequency and risk analysis in hydrology*. 4th Printing. Water Resources Publications. Fort Collins, Colorado. USA. 1988**;** pp. 4-26.
10. Bobée, B., Ashkar, F. *The Gamma family and derived distributions applied in Hydrology*. Water Resources Publications. Colorado, USA. 1991; pp. 121-161**.**
11. Rosbjerg, D. Prediction of floods in ungauged basins, in Runoff Prediction in Ungauged Basins. A Synthesis Across Processes, Places and Scales, edited by G. Blöschl, M. Sivapalan, T. Wagener, A. Viglione, and H. Savenije. 2013**.** chap. 9, pp. 189–226, Cambridge Univ. Press, Cambridge, U. K. https://doi.org/10.1002/2014EO020025
12. Gaur, A., Gaur, A., Simonovic, S. Future changes in Flood Hazard s across Canada under a Changing Climate. *Water*, **2018**, 10, 1441
13. Liu, D.F., Xie, B.T., Li, H.J., Design Flood Volume of the Three Gorges Dam Project, Publisher: ASCE, *Journal of Hydrologic Engineering*, 01, **2011.** Volume 16, Issue 1, pages 71-80, DOI: 10.1061/(ASCE)HE.1943-5584.0000287
14. Favre, A.-C., El Adlouni, S., Perreault, L., Thiémonge, N., Bobée B. Multivariate hydrological frequency analysis using copulas, *Water Resour. Res*. **2004.** 40, W01101, doi:10.1029/2003WR002456
15. De Michele, C., Salvadori, G., Canossi, M., Petaccia, A., Rosso, R. Bivariate statistical approach to check adequacy of dam spillway, *Journal of Hydrologic Engineering*. **2005.** 10 (1), 50–57. doi:10.1061/(ASCE)1084-0699(2005)10:1(50).
16. Volpi, E., Fiori, A. Design event selection in bivariate hydrological frequency analysis, *Hydrological Sciences Journal*. **2012.** 57(8), 1506-1515, DOI: 10.1080/02626667.2012.726357
17. Brunner, M. I., Seibert, J., Favre, A.-C.. Bivariate return periods and their importance for flood peak and volume estimation, *Wire's Water*, **2016**. 3, 819–833, doi:10.1002/wat2.1173
18. Gaal, L., Szolgay, J., Bacigal, T., Kohnova, S., Hlavcova, K., Vyleta, R., Parajka, J., Bloschl, G. Similarity of empirical copulas of flood peak-volume relationships; a regional case study of North-West Austria. *Contributions to Geophysiscs and Geodesy*. **2016.** vol. 46, issue 3, p. 155-178.
19. Stojkovic, M., Prohaska, S., Zlatanovic, N. Estimation of flood frequencies from data sets with outliers using mixed distribution functions. *Journal of Applied Statistics*. **2017**. vol.44, issue 11, p, 2017-2035.
20. Kang, L., Jiang, S., Hu, X., Li, C. Evaluation of Return Period and Risk in Bivariate Non-Stationary Flood Frequency Analysis. *Water*. **2019.** 11(1), 79; https://doi.org/10.3390/w11010079

21. Brunner, M.I., Sikorska-Senoner, A.E. Dependence of flood peaks and volumes in modelled discharge time series: Effect of different uncertainty sources. *Journal of Hydrology*. **2019.** vol. 572, 620-629
22. Prohaska, S., Ilić, A. Ch. 8. Theoretical Design Hydrographs at the Hydrological Gauging Stations along the Danube River. *Flood regime of rivers in the Danube River basin*. Pekárová, P., Miklánek, P. (ed). IH SAS, CD ROM, Bratislava, Slovakia. 2019. 215 pp. + 450 pp.
23. Yue, S., Rasmussen, P. Bivariate frequency analysis: Discussion of some useful concepts in hydrological applications, *Hydrol. Processes*. **2002.** 16, 2881 – 2898
24. Salvadori, G., De Michele, C. Frequency analysis via copulas: theoretical aspects and applications to hydrological events. *Water Resources Research*. **2004.** 40, W12511, doi:10.1029/2004WR003133.
25. Chuntian, C., Chau, K.W., Chunping, O. Flood Control Management System for Reservoirs as Non-structural Measures. International Workshop on Non-structural Measures for Water Management Problems, London, Canada, October 2001, pages 109-120
26. Grimaldi, S., Serinaldi, F. Asymmetric copula in multivariate flood frequency analysis. *Advances in Water Resources*. **2006.** Vol. 29, issue 8, pages 1155-1167
27. Karmakar S, Simonovic S.P. Bivariate flood frequency analysis: Part1. Determination of marginals by parametric and nonparametric techniques. *Journal of Flood Risk Management*. **2008.** 1:190-200. DOI: 10.1111/j.1753-318X.2008.00022.x.
28. Li, T.; Guo, S.; Liu Z.; Xiong, L.; Yin, J. Bivariate design flood quantile selection using copulas. *Hydrology research*. **2017**, 48(4): 997-1013
29. Brunner, M. I., Viviroli, D., Sikorska, A. E., Vannier O., Favre A.-C., Seibert, J. Flood type specific construction of synthetic design hydrographs. *Water Resour. Res.* **2017.** 53,1390–1406, doi:10.1002/2016WR019535
30. Mazzorana ,B., Hubl, J., Fuchs, S. Improving risk assessment by defining consistent and reliable system scenarios. *Nat Hazards Earth Syst Sci.* **2009.** 9(1):145–159
31. Mazzorana, B., Comiti, F., Fuchs, S. A structured approach to enhance flood hazard assessment in mountain streams. *Nat Hazards*. **2013.** 67:991–1009, DOI 10.1007/s11069-011-9811-y
32. STAS 4068/1-82. Determination of maximum water discharges and volume of watercourses (in Romanian). Romanian Institute of Standardization. 1982.
33. Drobot, R., Dragia, A.F. Design Floods Obtained by Statistical Processing. 24th Congress on Large Dams. Q94. Kyoto, Japan, 2012.
34. Stănescu V.Al., Ungureanu, V., Mătreață, M. Regional analysis of the annual peak discharges in the Danube catchment. The Danube and its catchment – A hydrological monograph, Follow-up volume No.VII. 2004. Regional Cooperation of the Danube Countries, Bucharest, Romania.
35. Chow V.T., Maidment D., Mays L. Applied Hydrology. McGraw-Hill.1988. pp. 380-415
36. Naden, P.S. Analysis and use of peaks-over-threshold data in flood estimation. In: *Floods and Flood Management. Fluid Mechanics and its Applications*. Saul A.J. (eds). 1992. vol 15. Springer, Dordrecht. https://doi-org.am.e-nformation.ro/10.1007/978-94-011-1630-5_10
37. Maidment, D.R. Handbook of Hydrology. Frequency analysis of extreme events, McGraw-Hill, 1993. 18.12-18.13.
38. Malamoud, B.D., Turcotte, D.L. The applicability of power-law frequency statistics to floods. *Journal of Hydrology*. 322 **2006**. 168–180.
39. Leadbetter, M. R. On a basis for 'Peaks over Threshold' modeling. *Statistics and Probability Letters.* **1991**. 12 (4): 357–362. doi:10.1016/0167-7152(91)90107-3.
40. Bhunya,P.K., Singh, R.D., Berndtsson, R., Panda, S.N. Flood analysis using generalized logistic models in partial duration series. *Journal of Hydrology.* **2012**. 420-421, pages 59-71
41. Ouarda, T.B.M.J., Cunderlik, J.M., St-Hilaire, A., Barbet, M., Bruneau, P., Bobée, B. Data-based comparison of seasonality-based regional flood frequency methods. *Journal of Hydrology*. **2006.** 330, 329– 339
42. Bezak, N., Brilly, M., Šraj, M. Comparison between the peaks-over-threshold method and the annual maximum method for flood frequency analysis. *Hydrological Sciences Journal.* **2014**. Vol. 59, No. 5, 959-977. https://doi.org/10.1080/02626667.2013.831174
43. Razmi, A., Golian, S., Zahmatkesh, Z. Non-Stationary Frequency Analysis of Extreme Water Level: Application of Annual Maximum Series and Peak-over Threshold Approaches. *Water Resour Management*. **2017.** 31:2065–2083.
44. Meylan, P., Favre, A.C., Musy, A. Hydrologie fréquentielle. Une science prédictive. Presses Polytechniques et Universitaires Romandes. 2008; pp. 137-159.
45. Pettit, A. N. A non-parametric approach to the changepoint problem. *Appl. Stat*. **1979.** 28, 126-135.
46. Ang A. H-S., Tang W. H. Probability Concepts in Engineering, Emphasis on Application to Civil and Environmental Engineering, 2nd Edition. John Wiley & Sons. 2006; 432 pages.
47. Bobée B., Cavadias G., Ashkar F., Bernier J., Rasmussen P. Towards a systematic approach to comparing distributions used in flood frequency analysis. *Journal of Hydrology.* **1993.** vol. 142, issues 1–4, pp 121–136
48. Koutsoyiannis, D. Uncertainty, entropy, scaling and hydrological statistics. 1. Marginal distributional properties of hydrological processes and state scaling / Incertitude, entropie, effet d'échelle et propriétés stochastiques hydrologiques. 1. Propriétés distributionnelles marginales des processus hydrologiques et échelle d'état, *Hydrological Sciences Journal*, **2005.** 50(3), 381-404
49. El Adlouni S., Bobée, B., Ouarda T.B.M.J. On the tails of extreme event distributions in hydrology. *Journal of Hydrology*. **2008.** vol. 355, issues 1–4, pp 16–33
50. Shanin M., Van Oorschoft H.J.L., De Lange S.J. Statistical Analysis in Water Resources Engineering. Balkema. 1993; pp. 81-125
51. Guo, S.; Muhammad, R.; Liu, Z.; Xiong F.; Yin, J. Design flood estimation methods for cascade reservoirs based on copulas. *Water*. **2018.** 10, 560; doi:10.3390/w10050560

52. Yin, J.; Guo, S; Liu, Z. Uncertainty analysis of bivariate design flood estimation and its impact on reservoir routing. *Water Resources Management*, **2018**, 32:1795-189
53. Bačová-Mitková, V., Onderka, M. Analysis of extreme hydrological Events on the Danube using the Peak Over Threshold method. *Journal of Hydrology and Hydromechanics*. **2010.** Volume 58: Issue 2 DOI: https://doi.org/10.2478/v10098-010-0009-x
54. Pekárová, P., Miklánek, P. (ed). Flood regime of rivers in the Danube River basin, the Danube and its tributaries – Hydrological Monograph Follow-up Volume IX. IH SAS, Bratislava, Slovakia. 2019. CD ROM, 215 pp. + 450 pp Annexes
55. Merz B., Thieken A.H. Flood risk curves and uncertainty bounds. *Natural Hazards*. **2009.** vol. 51, issue 3, p. 437-458, 2009 DOI: 10.1007/s11069-009-9452-6
56. Kundzewicz, Z. W., Robson A. J. Change detection in hydrological records—a review of the methodology / Revue méthodologique de la détection de changements dans les chroniques hydrologiques, *Hydrological Sciences Journal*. **2004.** 49:1, 7-19, DOI: 10.1623/hysj.49.1.7.53993
57. Hoffman, F.O., Hammonds, J.S. Propagation of uncertainty in risk assessments: the need to distinguish between uncertainty due to lack of knowledge and uncertainty due to variability. *Risk Anal*. **1994.** 14(5):707–712
58. Apel, H., Thieken, A. H., Merz, B., Bloschl, G. Flood risk assessment and associated uncertainty. *Natural Hazards and Earth System Sciences*, **2004.** 4: 295–308
59. Gericke, O.J., du Plessis, J.A. Evaluation of the standard design flood method in selected basins in South Africa, SAICE-SAISI, *Journal of the South African Institution of Civil Engineering*, **2012.** Volume 54, Issue 2, Pages 2 – 14
60. Darch, G.J.C., Jones, P.D. Design flood flows with climate change: method and limitations, Proceedings of the Institution of Civil Engineers-Water Management, 2012. vol. 165, issue 10, pages: 553-565, DOI: 10.1680/wama.12.00024
61. Pekárová, P., Miklánek, P., Bálint, G., Belz, J.U., Biondić, D., Gorbachova,L., Kobold, M., Kupusović, E., Soukalová, E., Prohaska, S., Škoda, P., Stanzel, P., Teodor S. Ch. 1 Average daily discharge and annual peak discharge series collection. In: Pekárová, P., Miklánek, P. (ed): Flood regime of rivers in the Danube River basin. IH SAS, 2019. CD ROM, Bratislava, 215 pp. + 450 pp Annexe
62. Apel, H., Merz, B., Thieken, A.H. Influence of dike breaches on flood frequency estimation. *Computers & Geosciences*. **2009.** 35, 907–923
63. FISRWG - Federal Interagency Stream Restoration Working Group. Stream corridor restoration: principles, processes and practices. National Technical Information Service, U.S. Department of Commerce, Springfield, VA. 1998.
64. Lang, M., Ouarda, T.B.M.J., Bobée, B. Towards operational guidelines for over-threshold modeling. *Journal of Hydrology*. **1999.** 225, 103–117
65. Bayliss, A.C. Deriving flood peak data. Flood Estimation Handbook. 1999. Vol. 3, p.273-283
66. Svensson, C.; Kundzewicz, Z., W.; Maurer, T. Trend detection in river flow series: 2. Flood and low-flow index series / Détection de tendance dans des séries de débit fluvial: 2. Séries d'indices de crue et d'étiage, *Hydrological Sciences Journal*. **2005.** 50:5, -824, DOI: 10.1623/hysj.2005.50.5.811
67. Šraj, M., Bezak, N., Brilly, M.. Bivariate flood frequency analysis using the copula function: a case study of the Litija station on the Sava River. *Hydrol. Process*. **2015.** 29, 225-238, (2015). DOI: 10.1002/hyp.10145
68. https://environmentalrisks.danube-region.eu/projects/danube-floodrisk /
69. EASTAVERT PROJECT "The prevention and protection against floods in the upper Siret and Prut River
70. IUGG. Contributions to Hydrological Sciences, 2012-2015. Ch. 2.7. Statistical Hydrology, pages 194-195
71. Wasko C, Westra S, Nathan R, Orr HG, Villarini G, Villalobos Herrera R, Fowler HJ. Incorporating climate change in flood estimation guidance. *Phil. Trans. R. Soc.* **2021**. A 379: 20190548. https://doi.org/10.1098/rsta.2019.0548
72. Serinaldi F, Kilsby CG. Stationarity is undead: uncertainty dominates the distribution of extremes. *Adv. Water Resour.* **2015**. 77, 17–36. doi:10.1016/j.advwatres.2014.12.013